Universal Arc Representation Using EMTP

Hatem A. Darwish and Nagy I. Elkalashy

***Abstract*—A preliminary description of a new arc representation has been introduced in [1]. In which, the Modified Mayr ($P-\tau$ model) arc equations are solved in the transient analysis control system (TACS) field of the electromagnetic transient program (EMTP) and represented in the power network by TACS controlled voltage source. In this paper, substantial improvements of this representation are carried out. A performance comparison with the EMTP built-in Avdonin model is incorporated to validate the proposed representation effectiveness. SF6 breakers with experimentally defined arc parameters are used to perform this comparison. The thermal limiting curve is computed by the proposed and the built-in models and compared with the measured characteristic. Also, universality of representation is verified via carrying out different arc model examples of circuit breaker and transmission-line arcing faults. The study results validated the proposed representation regarding accuracy and universality.**

***Index Terms*—Arc interaction, arc models, electromagnetic transient program (EMTP) simulation, Modified Mayr equation, system transients.**

I. Introduction

DESIGN of a circuit-breaker interrupting unit has been emphasized by several studies over the past years. Most of these studies have experimental nature, as the early breaker arc models have not produced satisfactory results for the manufacturers. Therefore, interrupter design was usually processed and optimized via series of laboratory tests in spite of the associated technical and economical sophistication. In order to overcome the experimental sophistication, efficient arc models should be developed to facilitate the evaluation of the interruption performance of the breaker. Modern breaker arc models have shown distinguished performance and numerous models are considered an important design aid particularly with initial design of the interrupting units [2]–[6].

Breaker arc models can be classified into three categories. Thermal and dielectric recovery models that describe the arc dynamical behavior considering the impact of different interrupter parameters such as nozzle size and geometry, type of quenching medium and speed of flow, pressure, ... etc. [2], [3]. Other models are based on empirical form(s) [4]. Both categories are efficient in determining the internal dimensions and quenching medium parameters of the interrupter. However, the third category of models is concerned with the arc external characteristics such as Cassie, and Mayr [5]–[9]. Unfortunately, arc modeling using either Cassie or Mayr equation only has not shown sufficient agreement for quantitative calculation over the whole current-zero period. Thus, combined Cassie-Mayr, Modified Mayr, and cascaded models are introduced. In cascaded arc models, the arc is divided into either two or three series parts. Each part is represented by a separate model [7]–[9]. It is reported that shortly before current zero, the contribution of the arc portion modeled by Mayr equation to the arc voltage is increased while the other portion modeled by Cassie goes to zero. Adversely, Cassie potion is dominating at high current periods. In sympathy with the series model, adaptive KEMA model that accounts for arc process at different periods is also introduced [10]. It can be concluded that models describing external arc characteristics is recommended, as far as investigation of breaker performance in the power system is only concerned. This may explain why three models from this category have been exclusively included in the electromagnetic transient program (EMTP) package [11].

Unfortunately, breaker arc card and card structure of version 2.0 of the EMTP was inadequate to fulfill different applications. Therefore numerous papers have proposed new models/representations that can be implemented in the EMTP environment [10]–[16]. These representations have better performance than that of the built-in ones. However, these representation may be implemented only in the Alternative Transient Program (ATP) or requires manufacturing data, which may not be available to the most of the users. Recently, the shortcomings of version 2 have been partially rectified with version 3.x of the EMTP [11]. Although models of version 3.x show improved accuracy, flexibility to account for universal applications is missed. For example arcing fault, arc furnace, empirical forms, innovations in arc models ... etc. are not directly implemented in version 3.x. This can be remedied with the proposed arc representation [1]. Although this primary representation accounted for $P-\tau$ model only, additional efforts are directed for further enhancement toward universality [17].

In this paper, a universal breaker arc representation in the form of controlled voltage source in the EMTP is presented. A comparison of the proposed representation with the EMTP built-in Avdonin model is performed. Thermal limiting curve derivation and breaker performance evaluation in a direct test circuit, short line fault (SLF) circuit, and transmission system are carried out. Possibility of implementing different arc models using the novel representation is also investigated.

II. Proposed Arc Representation

The proposed representation of the arc model can be explained with the help of Fig. 1. The generator is used to provide the breaker with the short circuit current level and the $\mathrm{R_c}-\mathrm{C_c}$ branch is used to control the rate of rise of the recovery voltage (RRRV). The breaker arc is represented by transient analysis control system (TACS)-controlled voltage source type 60. The value of the voltage is computed in the TACS field

Manuscript received July 28, 2003; revised April 9, 2004. Paper no. TPWRD-00397-2003.

The authors are with Power System Protection Group (PSPG), Department of Electrical Engineering, Faculty of Engineering, Menoufiya University Shebin, Elkom 32511, Egypt (e-mail: h_a_darwish@yahoo.com).

Digital Object Identifier 10.1109/TPWRD.2004.838462

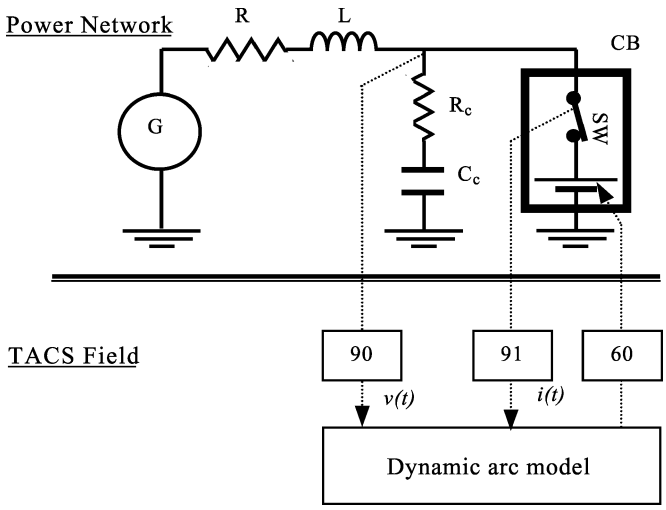

Fig. 1. EMTP network of synthesizer generator and breaker.

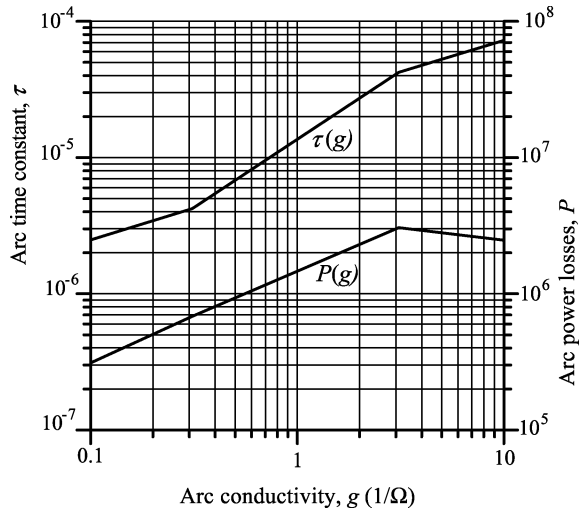

Fig. 2. Reported $P-\tau$ functions of the circuit breaker [6].

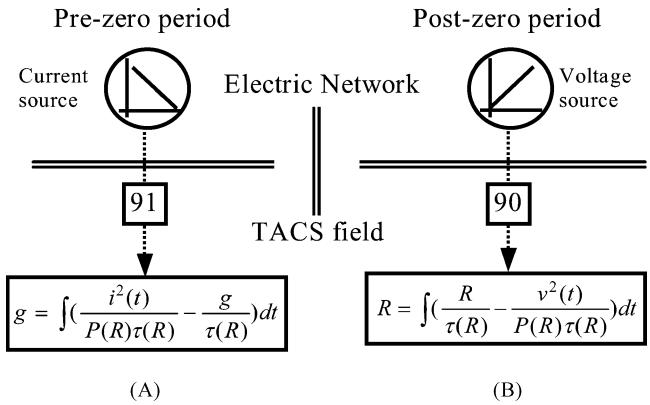

Fig. 3. Proposed technique for computing thermal limiting curve. (a) Arc conductivity; (b) critical RRRV.

by multiplying the computed arc resistance by the arc current measured by sensor 91. This resistance is derived from the dynamic arc equation(s) exploiting the TACS tools. At the next step, the corresponding arc voltage can be fed back into power network via controlled voltage source type 60. In this manner, arc interaction with the power system elements is fully considered. Note that during pre-zero current periods, the controlled voltage source is connected to the system, as the switch SW is normally closed until current zero crossing. While for testing the breaker RRRV withstanding during post current-zero interval, the switch is opened and the breaker voltage is transported into TACS field by sensors 90. Then, the RRRV against the zero current conductivity states interruption/re-ignition conditions according to post zero dynamic arc equation(s). Control signals are generated in order to distinguish between the pre and post zero current periods. Details of the $P-\tau$ model implemented using this universal representation is given in [1] and summarized in the Appendix.

Some efforts have been directed to improve this model performance. These efforts include elimination of numerical instability that may be produced due to the wide difference between the power system and arc time constants considering the solution time step (Δt). Also, representation of the contact parting interval is considered. The vital enhancement is the added adaptability of the representation to realize different arc models considering EMTP version 2.0 environment or higher. The later is investigated with examples in Section V.

III. Thermal Limiting Curve

An SF6 breaker rated at 123-kV and 40-kA breaking current is used as a test sample [6]. In which, the characteristic arc time constant $\tau(g)$ and power loss $P(g)$ functions were obtained experimentally via series of short circuit tests as given by Fig. 2 [6]. It is obvious from Fig. 2 that, $P(g)$ and $\tau(g)$ functions are divided into three functions considering the magnitude of the conductivity (g). This would represent an obstacle to EMTP Avdonin model as this model accounts only for a single function of $P(g)$ and $\tau(g)$.

A. Limiting Curve Using the Universal Representation

Thermal limiting curves are usually extracted using the synthesizer generator tester shown in Fig. 1. The tester is usually considered as stiff current and voltage sources for pre and post-zero crossings, respectively. Thus, EMTP network given by Fig. 1 can be easily reduced to a simpler network as shown in Fig. 3. The network current and voltage are used as inputs to the first order differential equations of modified Mayr as

$$g = \int \left(\frac{i^2(t)}{P(R)\tau(R)} - \frac{g}{\tau(R)} \right) dt \tag{1}$$

$$R = \int \left(\frac{R}{\tau(R)} - \frac{v^2(t)}{P(R)\tau(R)} \right) dt \tag{2}$$

where $i(t)$ is the arc current, $v(t)$ is the arc voltage, R is the arc resistance, $R = 1/g$, $\tau(R) = \tau_o R^{\alpha}$ is the arc time constant, $P(R) = P_o R^{\beta}$ is the arc power losses and α and β are constants. Note that, the modified Mayr model is given here for demonstration purposes only.

The three $P(g)$ and $\tau(g)$ functions of Fig. 2 are realized in the EMTP considering the flexibility of TACS FORTRAN expressions. The measured current is used as an input to (1) during the pre-zero crossing while the arc voltage is considered as an input to (2) during post-zero crossing, as shown in Fig. 3. In Fig. 3(a),

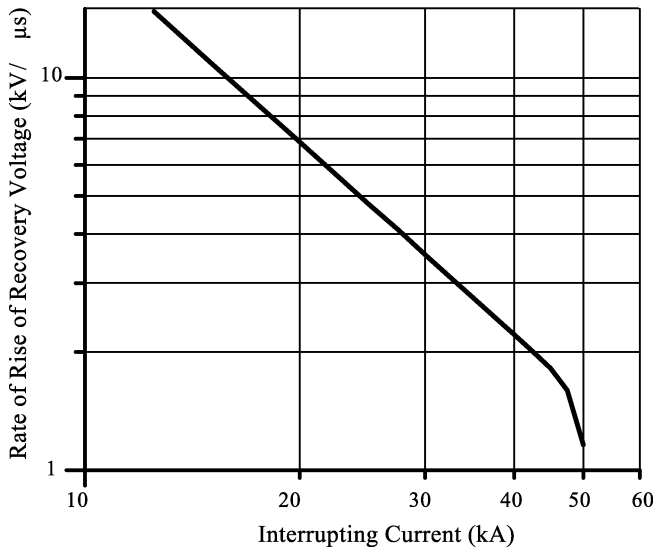

Fig. 4. Limiting curve using the universal arc representation.

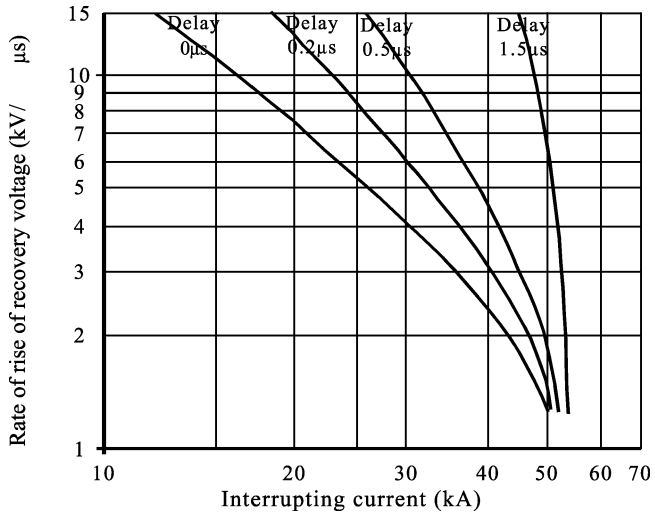

Fig. 5. Reported thermal limiting curves [6].

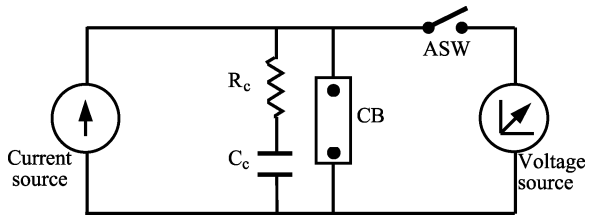

Fig. 6. Test circuit for carrying out the built-in thermal characteristic curve.

the arc conductivity can be computed at zero crossing against the interrupting current (I) by applying different values of the current from the power network fed the integral form of (1) in the TACS field. Thereafter, the value of g at the zero crossing is utilized as an initial condition for arc dielectric recovery described by a different DAT file. This file is developed for carrying out the RRRV limits during post-zero crossing as shown in Fig. 3(b). The stiff voltage source is represented by a source card with constant ramp value and excites the integral form of (2). This equation is tested for different values of the RRRV for estimating the critical RRRV limit. By combining both results of pre and post-zero crossings, the RRRV-I limiting curve can be deduced to explore the breaker thermal failure limits as shown in Fig. 4. It is evident from Fig. 4 that a good matching between the computed and the reported thermal limiting curve that traced by Fig. 5 for zero time delay of voltage application on the arc channel post current zero. Note that, the curves shown in Fig. 5 are experimentally obtained as reported in [6]. Different delay times account for a free interval of conductivity decaying before the application of RRRV.

B. Limiting Curve Using EMTP Avdonin Model

Avdonin arc model is one of the breaker models in the EMTP and it is defined by arc voltage, arc time, parting time, node names, and the arc model parameters considering the following equation [7]:

$$\frac{1}{R}\frac{dR}{dt} = \frac{1}{\tau(R)}\left(1 - \frac{v(t)\times i(t)}{P(R)}\right). \tag{3}$$

Deducing the limiting curves using Avdonin model is not an easy task. This is because it is not possible to measure the arc conductivity at zero crossing with this built-in model format. That is in order to test it with different RRRV until obtaining the critical level. The test circuit shown by Fig. 6 is proposed to overcome this issue. The circuit consists of current source with negative $\mathrm{d}i/\mathrm{d}t$ during the pre-zero crossing, while for post-zero region a variable voltage source with constant ramp value of RRRV is applied. The values of $\mathrm{R_c} - \mathrm{C_c}$ are selected such that minimal deformations, as possible, on the breaker $\mathrm{d}i/\mathrm{d}t$ and RRRV nearby the zero crossing point are produced. In which, reducing capacitor size and increasing the resistor would reduce the deformation in $\mathrm{d}i/\mathrm{d}t$ and RRRV. However, with R_c values over 10 kΩ and C_c below 10^{-5} μF, numerical instabilities have been recorded due to the produced low time constant values and the associated Δt. Therefore, these values are considered as the $\mathrm{R_c} - \mathrm{C_c}$ limits. Also, the instant of closing the switch ASW is set equal to the starting time of the voltage source. This instant should be declared in the source card. In order to reduce the associated error, the selected Δt for the numerical solution should be as small as possible.

Another issue is raised with the application of this particular breaker test sample. The breaker has three functions of $P(R)$ and $\tau(R)$ considering arc resistance value. Declaring these functions is impossible considering EMTP Avidonin model cards. In order to sort out this issue, two solutions are proposed. The first one is to use $P(R)$ and $\tau(R)$ corresponding to the lowest value of g and use them in the declaration of the arc parameter card. The other solution is to use some regression forms in order to reduce the three functions into single function. The first solution is applied and the limiting curve is computed as shown in Fig. 7. It is evident from Fig. 7 that the derived curve by the built-in model has a lower accuracy than that of the universal representation. The inaccuracy is progressively increased with the increase of the interrupted current toward levels higher than 46 kA. This is attributed to the flexibility of the proposed representation in considering the three functions of $P(g)$ and $\tau(g)$ compared with only one function is declared in the built-in Avdonin model.

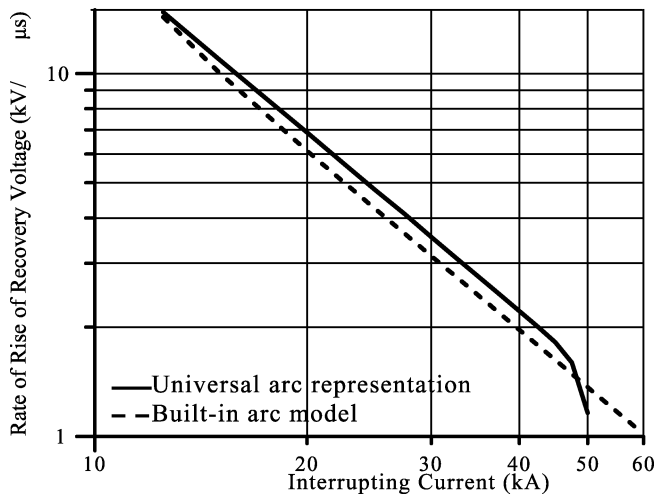

Fig. 7. Comparison of the computed limiting curves.

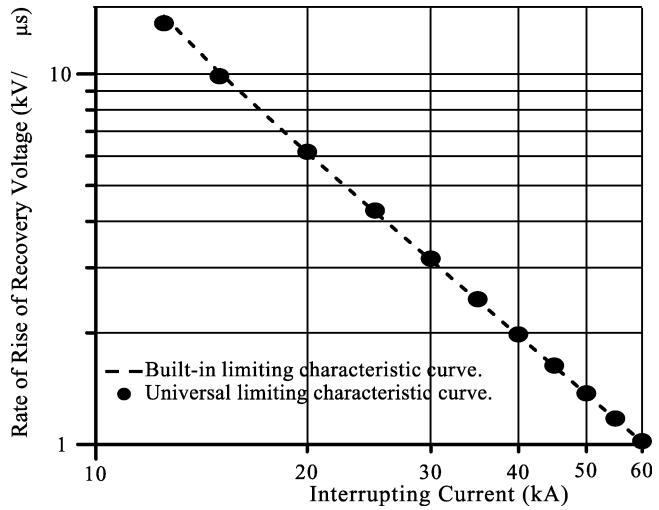

Fig. 8. Thermal limiting curves of the two models for the same arc parameters.

In order to confirm the aforementioned conclusion, a single function of $P(g)$ and $\tau(g)$ is considered for the proposed representation and Avdonin built-in models. Then, the thermal limiting curves are computed, as shown in Fig. 8. The results of both models are fairly close, however both curves are relatively deviated from the reported limiting curve of Fig. 5. This would reveal that the proposed representation has the same accuracy of the built in models as far as single function for $P(g)$ and $\tau(g)$ is considered. However, the proposed representation has the advantage of flexible consideration of multi functions defining $P(g)$ and $\tau(g)$. It is to be also noted that the curve of zero time delay is only considered in the comparison. Other curves with different time delays cannot be considered as the built-in model format does not fulfill such conditions.

IV. Comparison Using Direct Test Systems

Testing of hvac circuit breakers using the laboratory direct test circuit is extremely difficult. Where, one source delivers the required current under the specified voltage as shown in Fig. 1. The EMTP network equivalent to the synthesizer generator of

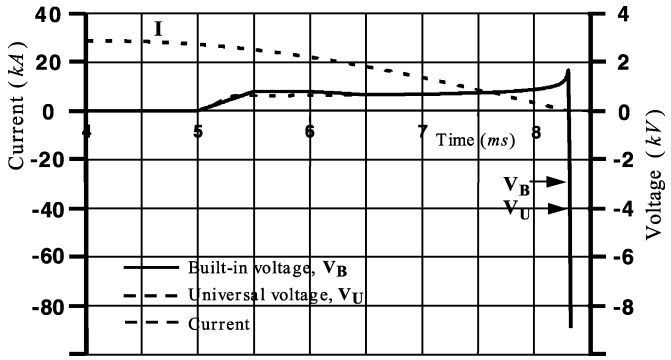

Fig. 9. Arc voltage comparison using direct test circuit.

Fig. 1 can be deduced without the consideration of the aforementioned simplifications (stiff current and voltage sources for pre and post-zero crossing, respectively). In this case, one DAT file program should handle both periods. For carrying out the computation study, the voltage source of Fig. 1 is selected with 106.14 kV peak, 0° angle, and 60 Hz frequency [16]. The $R_c - C_c$ branch is 57.38 Ω and 1.055 μF, respectively [18]. The values R and L are 0.0 Ω and 9.8 mH, respectively.

The breaker is represented at first with Avdonin model. In which, the circuit breaker starts parting its contacts at 5 ms, starting time of arc voltage Tmax is 5.5 ms with Vmax of 800 V, and the arcing time is declared by 6.0 ms, from the program starting time. However for the universal representation, the same EMTP network with Avdonin cards is considered but with the replacement of Avdonin model by the proposed one. After the breaker is opened, the dynamic arc equations are solved, arc voltage is computed, and then passed back to the network. This will produce sudden change in voltage and may lead to numerical instability. In order to overcome this drawback, the controlled voltage source is set similar to the built-in model with constant ramp value representing the contact parting. Thereafter, the arc voltage is computed by solving the integral forms of the dynamic arc equations with consideration of the arc interaction. Fig. 9 shows the measured arc voltage using Avdonin and the universal arc representation. It is evident from Fig. 9 that, both time responses have exact-matching in the vicinity of the current zero. However, a slightly different behavior in the representation of contact parting as the proposed representation considers arc voltage building up with constant rate of 2.0 kV/ms until reaching the estimated value by the dynamic arc equation.

On the other hand, testing both models is also performed considering the power transmission system shown in Fig. 10. Parameters of this transmission system are given in [19] and used in the paper but for 110-kV bus voltage. The following scenario is considered, at 32 ms a line-to-ground fault is occurred at the end of the 15 miles-transmission line. Consequently, the protection relays trip breaker CB1, which is represented by the SF6 breaker test sample. At 42 ms, the contacts of the breaker are separated and the arc is created. From this instant and until the arc extinction, the potential difference between BUS1 and BRK1 is forced from the TACS field via the controlled voltage source. This represents a challenge in the EMTP, as the voltage source must be connected to one node name only according to the EMTP rulebook [11]. In order to sort out this problem,

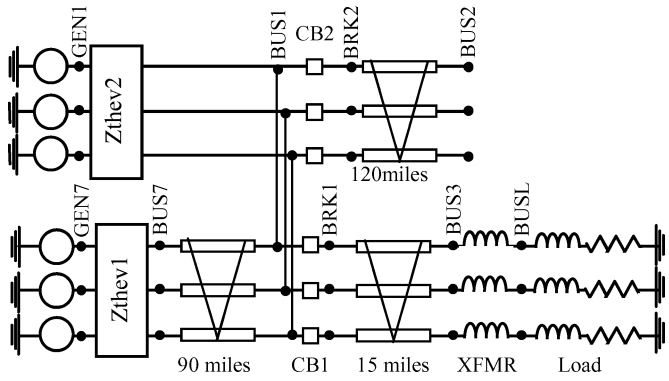

Fig. 10. Transmission line network.

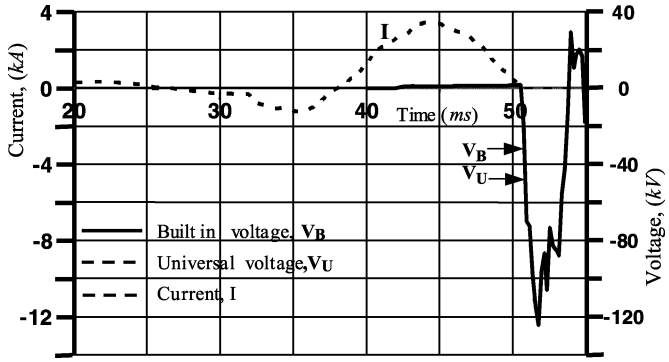

Fig. 11. Arc voltage comparison in transmission line.

the controlled voltage source is replaced by two controlled current sources injecting current (I) and (-I) in a small resistance connected in series with the network. The produced voltage drop across the resistor is equal to the voltage of the controlled voltage source. Fig. 11 shows the performance of the proposed and the Avdonin representation of the modified Mayr arc model. It is evident from Fig. 11 that excellent matching between both responses is obtained.

V. Representation Universality

A. The Representation of Improved Mayr Model

One of the innovations in arc models is the Improved Mayr model, which is introduced by KEMA High Power Laboratory Group [10]. Although, this model cannot be realized considering built-in models, it can be implemented using the proposed representation. This adaptive arc model is given by

$$g = \int \frac{1}{\tau}\left(\frac{i^2}{\max\left(U_{arc}|i|, P_o + P_1 v.i\right)} - g\right) dt \qquad (4)$$

where P_1 and P_o are constants of cooling power and τ is the arc time constant. However, U_{arc} is the constant arc voltage in the high current area. Equation (4) is used to represent the dynamic arc equation during pre-zero current period. In which, model conformity with Cassie in high current area is fulfilled. However, Improved KEMA model has constant cooling power, which is dominant near current zero area. This is fulfilled by the

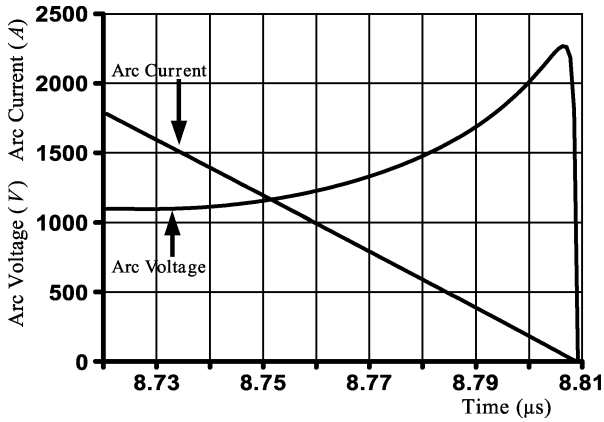

Fig. 12. Arc current and voltage traces using the SLF test circuit.

max statement of (4). After current zero, the equation is reduced to the Mayr arc model as

$$R = \int \frac{1}{\tau}\left(R - \frac{v^2}{P_o}\right) dt. \qquad (5)$$

The proposed universal representation is adapted to account for KEMA model by replacing (1) with (4) in TACS field during the pre-zero current period. While the arc expression of (5) is implemented instead of (2) for testing the breaker recovery withstanding during post-zero current interval. These modifications are only incorporated without altering the other universal representation blocks or signals in both power and TACS network. In brief, arc expressions are only altered, keeping the same EMTP network of Fig. 1, to account for the implementation of Improved Mayr model using the proposed universal arc representation.

Two SF6 breakers rated at 245 kV/50 kA/50 Hz are used as test example. The arc parameters of the breakers required by the Improved Mayr model are considered. The parameters of the first one are: $\tau = 0.27\ \mu$s, $P_o = 15\,917$, $P_1 = 0.9943$, and $U_{arc} = 100$ V while for the second breaker: $\tau = 0.57\ \mu$s, $P_o = 24\,281$, $P_1 = 0.9942$, and $U_{arc} = 1135$ V. These values have been obtained from the least square fit of KEMA experimental results [10].

The proposed arc representation can be validated by recognizing the computed waveforms of arc voltage and current in vicinity of current zero when the breaker is tested through short line fault (SLF) test circuit. In which the aforementioned circuit breakers are tested in practical test circuits used by KEMA (90% SLF test) [10]. When the two breakers are tested using the universal arc representation, the first one has successful interruption while the second has re-ignition state and their voltage and current waveforms in the vicinity of zero-current are depicted in Figs. 12 and 13 respectively. These waveforms present perfect match to the measured waveforms reported in [10]. This insures the efficiency of the proposed arc representation.

In addition, the real time operation of the first breaker can be evaluated with the help of the transmission system given in Fig. 10. However, the system bus voltage is adjusted to 230 kV. The breaker parameters are as described in this section and arc voltage is declared with approximately 1100 V in high current area. The time response of the breaker is shown in Fig. 14 for

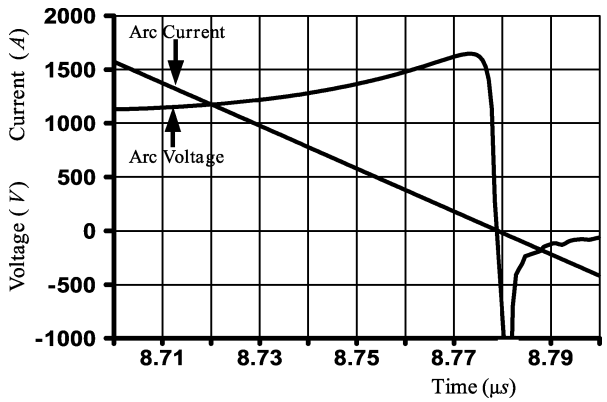

Fig. 13. Arc current and voltage for a reignition using the SLF test circuit.

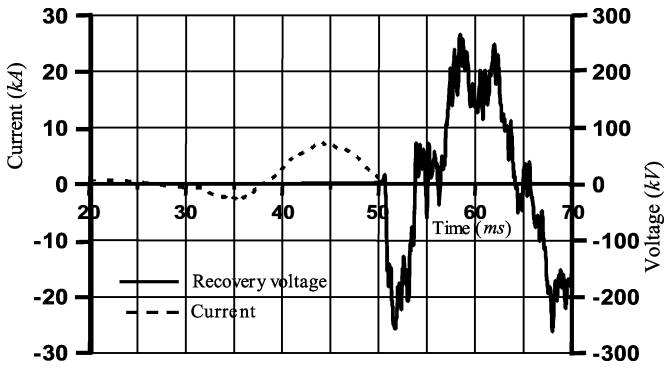

Fig. 14. Real-time operation of ac breaker.

the same scenario described in Section IV. It is found that the arc voltage in the high current area is close to the specified one by the model data which reflects the conformity with Cassie model, while near zero point the improved Mayr model with its three free parameter is ruling the arc performance. This result insures the universality of the proposed arc representation as it can be easily altered to suit other arc models and conditions such as transmission-line arcing faults.

B. Representation of Series Arc Models

For this type of models, the arc is divided into a series connection of two parts; one is described by Cassie equation and the other by Mayr as [7]

$$\frac{1}{g_c}\frac{dg_c}{dt} = \frac{1}{\tau_c}\left(\frac{i^2(t)}{U_c^2 g_c^2} - 1\right) \tag{6}$$

$$\frac{1}{g_M}\frac{dg_M}{dt} = \frac{1}{\tau_M}\left(\frac{i^2(t)}{P_o g_M} - 1\right) \tag{7}$$

$$\frac{1}{g} = \frac{1}{g_c} + \frac{1}{g_M} \tag{8}$$

where g_c and g_M are the conductivity of the Cassie and Mayr part of the arc, respectively. At high currents, most of the voltage drops takes place in the Cassie portion. Shortly before current zero the contribution the Mayr equation increases rapidly, then, its withstanding of the recovery voltage after current zero can be examined.

The possibility of representing the four constant parameters model using the universal arc representation in SLF test circuit is also considered, the curve of ratio of constant rate of change

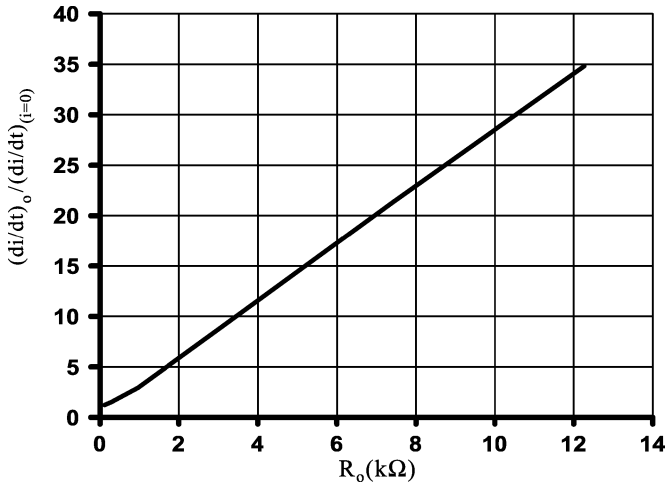

Fig. 15. Relative rate of arc current $(di/dt)_o/(di/dt)_{i=0}$ as a function of $\mathrm{R_o}$.

of current at an interval of 5 μs before current zero $(di/dt)_o$ to its value at current zero $(di/dt)_{i=0}$ (or $(di/dt)_o/(di/dt)_{i=0}$) against the arc resistance at zero crossing R_o is carried out as shown in Fig. 15. In which the four parameters are selected within the described range reported in [8]. Alikeness of the obtained curve with the reported one in [8] supports the universality of proposed arc implementations.

C. Representation of Arcing Faults

Transmission line arcing faults are widely experienced in power system and usually categorized as transient faults. Modeling of arcing faults and its interaction with the power system is important for designing and testing the protection relays. Also, classifying these types of faults would enhance the operation of extra high voltage autoreclosures. One of the widely used models for representing the arcing faults is the thermal model of M. Kizilcay [14]. In which, a synthetic test circuit is developed to obtain the parameters of primary and secondary phases of the arc along a 380-kV insulation string. The arcing fault equation of Kizilcay model is given as

$$g = \int \frac{1}{\tau}(G - g)dt \tag{9}$$

$$G = \frac{|i|}{u_{st}} \tag{10}$$

$$u_{st} = (u_o + r|i|)\,l \tag{11}$$

where g is time-varying arc conductance, G is stationary arc conductance, τ is arc time constant, r is the resistive component per arc length, u_o is constant voltage per arc length, l is time-dependent arc length, and i is arc current. Primary arc parameters are: l is 350 cm, τ is 1.3 ms, u_o is 12 V/cm, and r is 1.3 $\mathrm{m\Omega/cm}$. The secondary arc parameters are considered as given in [14].

For representation of the fault arcs using the universal representation, the breaker arc equations are replaced by Kizilcay model similar to KEMA model described in the previous section. Furthermore, control signals are generated to distinguish between primary and secondary arc periods. This is to fulfill each period with its different arc parameters as described previously.

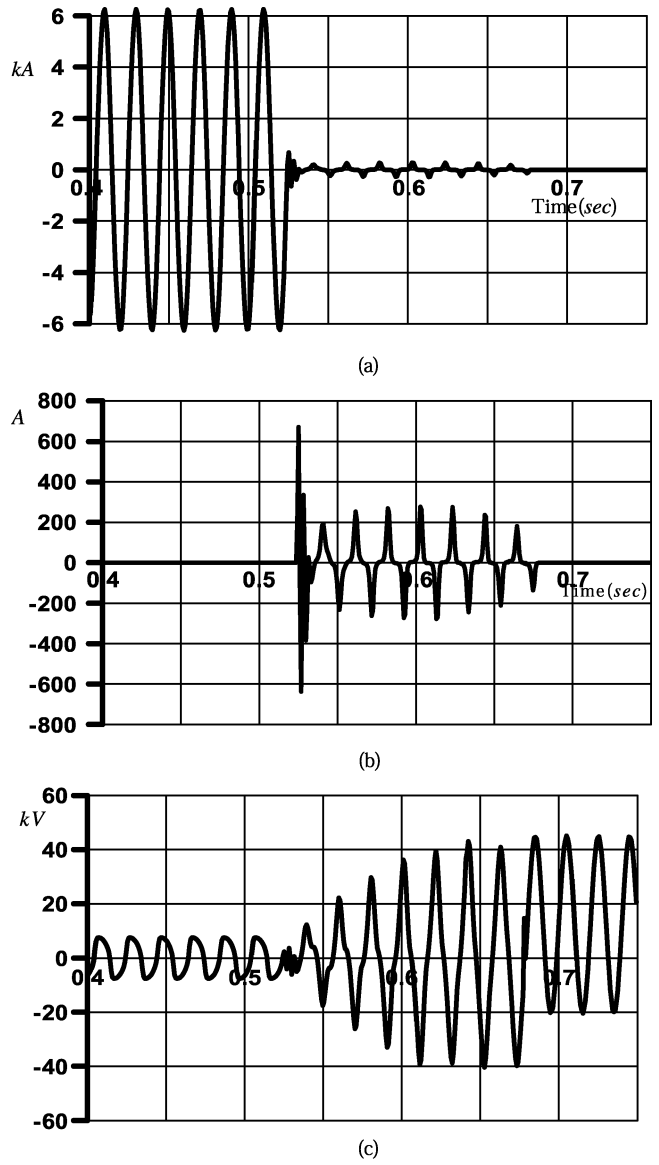

Fig. 16. Currents and voltage for primary and secondary arcing fault. (a) Arc current. (b) Secondary arc current. (c) Arc voltage.

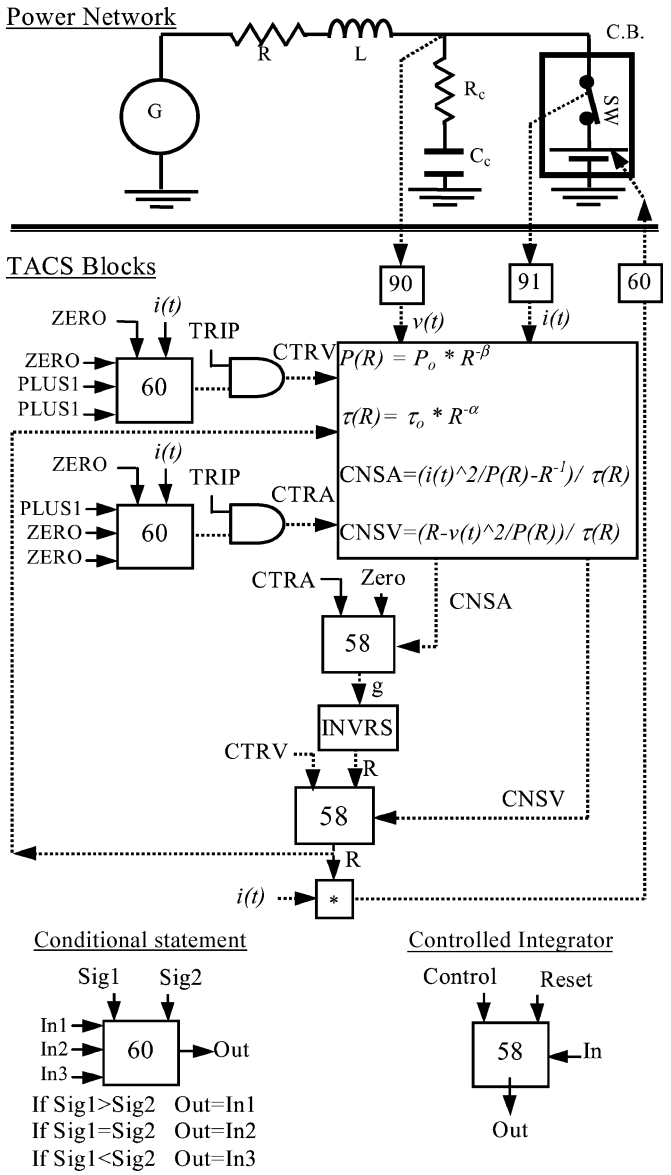

Fig. A.1. Universal arc representation of modified Mayr model.

The obtained currents and voltage of primary and secondary fault arc are depicted in Fig. 16. The computed results are identical to ones obtained by the experimental setup and the consecutive ATP simulation reported in [14], in which the dc offset of voltage waveforms shown in Fig. 16(c) is due to the capacitor residual charge. When the arc is extinguished, the residual charges voltage on the capacitor at this instant lead to this offset. The value of dc offset is dependent on extinction instant.

It is evident from the aforementioned investigation and comparisons that the proposed representation has shown the flexibility to accommodate different arc models in addition to the straightforward methodology in connecting or altering the arc element over the power system arrangement.

VI. Conclusion

A universal arc implementation in the EMTP environment has been validated via comparing the results with the built-in Avdonin model. The thermal limiting curves have been computed and the model results are deeply investigated. The investigation has been extended to cover the breaker operation in a direct test circuit, SLF test circuit and in a typical power transmission system. Possibility of implementing alternative arc models such as the Improved-Mayr (KEMA), cascaded arc, and arcing fault models has been studied and the simplicity of altering the proposed representation to account for different models is confirmed. The test results ultimately verify the universality and simplicity of proposed arc representation for miscellaneous application. It can be fairly said that the universal arc representation is considered as a new add-on card to the EMTP arc models.

Appendix

The proposed arc representation is depicted in Fig. A.1 [1]. The two integral forms of the modified Mayr model is combined in one arrangement. After breaker tripping, the arc is created.

The control signals CTRA and CTRV are generated by the assistance of the Logical FORTRAN expressions in order to distinguish the current pre and post-zero crossing periods. In pre-zero intervals, the signal CTRA is relatively high until current zero. However in the post-zero periods, the CTRV signal turns to high and CTRA is low. This is achieved using a conditional statement (device type 60) for comparing the arc current with zero value. The result of this device and the generated signal SIG0 are used as inputs for the AND gate which is represented by a supplemental variable using logical operators in the FORTRAN statement. The produced signals CTRA and CTRV are used as control signals for the two controlled integrators. When CTRA is high, (1) is solved for computing the arc conductivity during pre-zero periods. Consequently, the arc resistance is magnified by the arc current value to compute the arc voltage, which is fed back into the power network in the next time step. Also, the arc resistance is used in calculating $\tau(R)$ and $P(R)$. When the control signal CTRV is high, the value of the arc resistance at zero crossing is used as an initial condition for (2) during post-zero current. Consequently, the arc resistance can be computed and interruption/re-ignition of the breaker is obtained.

REFERENCES

[1] H. A. Darwish, M. A. Izzularab, and N. I. Elkalashy, "Implementation of circuit breaker arc model using electromagnetic transient program," in *Proc. 8th Middle-East Power Systems Conf.*, Egypt, 2001, pp. 809–814.

[2] H. J. Schoetzau, H. P. Meili, E. Fischer, C. Strurzenegger, and H. P. Graf, "Dielectric phase in an SF6 breaker," *IEEE Trans. Power App. Syst.*, vol. PAS-104, no. 7, pp. 1897–1902, Jul./Aug. 1985.

[3] K. Ragaller, A. Plessel, W. Herman, and W. Egli, "Calculation Methods for the Arc Quenching System of Gas Circuit Breaker," CIGRE-13.03, Paris, France, Aug. 29–Sep. 6, 1984.

[4] S. Taylor, B. Wang, T. R. Blackburn, and G. R. Jones, "Thermal Reignition Performance Limitation of a Modal SF6 Circuit Breaker Under Full and Scaled Power Conditions," Arc Resistance Rep., Univ. Liverpool, Liverpool, U.K., Electrical Eng., ULAP-T72, 1982.

[5] CIGRA Working Group 13.01, "Applications of black box modeling to circuit breakers," *Electra*, no. 149, Aug. 1993.

[6] M. Hrabovsky, V. Mastny, and Z. Vostracky, "Application of mathematical arc model for determination of thermal failure limiting characteristics," *CIGRE*, Aug. 29–Sep. 6, 1984.

[7] U. Habedank, "Application of a new arc model for the evaluation of short-circuit breaking tests," *IEEE Trans. Power Del.*, vol. 8, no. 4, pp. 1921–1925, Oct. 1993.

[8] U. Habedank and H. Knobloch, "Zero-crossing measurements as a tool in the development of high-voltage circuit breakers," *Proc. Inst. Elect. Eng., Sci. Meas. Technol.*, vol. 148, no. 6, pp. 268–272, Nov. 2001.

[9] R. Smeets and V. Kertesz, "Evaluation of high-voltage circuit breaker performance with a validated arc model," *Proc. Inst. Elect. Eng., Sci. Meas. Technol.*, vol. 147, no. 2, pp. 121–125, Mar. 2000.

[10] P. H. Schavemaker and L. Sluis, "An improved Mayr-type arc model based on current-zero measurements," *IEEE Trans. Power Del.*, vol. 15, no. 2, pp. 580–584, Apr. 2000.

[11] *Electromagnetic Transient Programs (EMTP96) Rule Book*.

[12] L. Van der Sluis, W. R. Rutgers, and C. G. A. Koreman, "A physical arc model for the simulation of current zero behavior of high-voltage breakers," *IEEE Trans. Power Del.*, vol. 7, no. 2, pp. 1016–1022, Apr. 1992.

[13] L. Van der Sluis and B. L. Sheng, "The influence of the arc voltage in synthetic test circuits," *IEEE Trans. Power Del.*, vol. 10, no. 1, pp. 174–279, Jan. 1995.

[14] M. Kizilcay and T. Pniok, "Digital simulation of fault arcs in power systems," *Eur. Trans. Electrical Power System, ETEP*, vol. 4, no. 3, pp. 55–59, Jan./Feb. 1991.

[15] S. Varadan, E. B. Makram, and A. A. Girgis, "A new time domain voltage source model for an arc furnace using EMTP," *IEEE Trans. Power Del.*, vol. 11, no. 3, pp. 1685–1691, Oct. 1996.

[16] V. Phaniraj and A. G. Phadke, "Modeling of circuit breakers in the electromagnetic transient program," *IEEE Trans. Power Syst.*, vol. 3, no. 2, pp. 799–805, May 1988.

[17] H. A. Darwish and N. I. Elkalashy, "Comparison of universal circuit breaker arc representation with EMTP built-in model," in *Proc. Int. Conf. Power System Transients*, New Orleans, LA.

[18] G. St-Jean and R. F. Wang, "Equivalence between direct and synthetic short-circuit interruption tests on HV circuit breakers," *IEEE Trans. Power App. Syst.*, vol. PAS-102, no. 7, pp. 1897–1902, Jul. 1983.

[19] F. L. Alvarado, R. H. Lasseter, and W. F. Long, Electromagnetic Transient Program (EMTP) Workbook, Univ. Wisconsin Madison, Sep. 1986.

Hatem A. Darwish was born in Quesna, Egypt on Sept. 13, 1966. He received the B.Sc. (Hons.), M.Sc., and Ph.D. degrees in electrical engineering, Menoufiya University, Egypt in 1988, 1992, and 1996, respectively. From 1994 to 1996, he was working toward the Ph.D. degree at Memorial University of Newfoundland, St. John's, Canada based on joint supervision with Menoufiya University.

He has been involved in several pilot projects for the Egyptian industry for the design and implementation of numerical relays, SCADA, fault location, and relay coordination. Dr. Darwish is currently an Associate Professor. His interests are in digital protection, signal processing, EMTP simulation, and system automation.

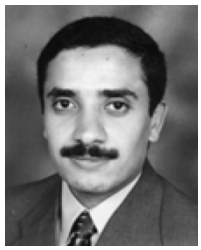

Nagy I. Elkalashy was born in Quesna, Egypt on August 4, 1974. He received the B.Sc. (Hons.) and M.Sc degrees from the Electrical Engineering Department, Faculty of Engineering, Shebin El-Kom, Menoufiya University in 1997 and 2002, respectively, where he is currently pursuing the Ph.D. degree.

His research interests include switchgear, EMTP simulation, and power system transient studies including AI.